Journal of Sound and Vibration (2001) **244**(2), 339–357
doi:10.1006/jsvi.2000.3498, available online at http://www.idealibrary.com on IDEAL®

CRACK IDENTIFICATION IN VIBRATING BEAMS USING THE ENERGY METHOD

X. F. YANG, A. S. J. SWAMIDAS AND R. SESHADRI

Faculty of Engineering and Applied Science, Memorial University of Newfoundland, St. John's, NF, Canada A1B 3X5

(*Received* 19 *January* 2000, *and in final form* 13 *November* 2000)

An energy-based numerical model is developed to investigate the influence of cracks on structural dynamic characteristics during the vibration of a beam with open crack(s). Upon the determination of strain energy in the cracked beam, the equivalent bending stiffness over the beam length is computed. The cracked beam is then taken as a continuous system with varying moment of intertia, and equations of transverse vibration are obtained for a rectangular beam containing one or two cracks. Galerkin's method is applied to solve for the frequencies and vibration modes. To identify the crack, the frequency contours with respect to crack depth and location are defined and plotted. The intersection of contours from different modes could be used to identify the crack location and depth.

1. INTRODUCTION

For vibration analyses of cracked beams and possible crack detection, the fracture mechanics procedure is generally preferred [1]. According to this procedure, the crack occurring in a beam would reduce the local stiffness at the location of the crack. In using the fracture mechanics model, the local stiffness is calculated using Castigliano's second theorem as applicable to fracture mechanics formulations. The calculated local stiffness is then modelled by a flexural spring for the bending vibration of a cracked beam. To establish the vibration equations, the cracked beam was represented by two substructures connected by a flexural spring. Irwin [2] was the first to relate the local flexibility of a cracked beam to the stress intensity factor. Okamura *et al.* [3] determined the local flexibility for the axial and bending behaviors in a rectangular beam, separately. They examined the variation of the first natural frequency of a free–free beam as a function of the crack depth. Ju *et al.* [4] considered a beam in pure bending and used the results in connection with damage detection. Dimarogonas and Paipetis [5] established a 5×5 flexibility matrix to model the vicinity of a crack; torsion was not included in the model. Later Papadopoulos and Dimarogonas [6] extended the matrix formulation by adding torsion resulting in a full 6×6 flexibility matrix. A comprehensive review on vibrations of cracked structures can be found in reference [7] by Dimarogonas.

Some researchers have used the variational principle to develop vibration equations for cracked beams. Christides and Barr [8] first proposed an exponential-type function (crack disturbance function) to model the stress/strain variation around the crack zone, in which one parameter was to be determined by experiments. Based on the assumed stress, strain and displacement expressions, the vibration equations of beams with symmetrical cracks

0022-460X/01/270339 + 19 $35.00/0

were derived using the Hu-Washizu variational principle. Shen *et al.* [9, 10] followed a similar procedure to investigate the vibration of cracked beams with single or symmetrical cracks, the solution to which was obtained using Galerkin's method with many terms. Recently, Chondros and Dimarogonas [11] have generated some solutions for the crack functions in vibrations of a cracked cantilever beam using the fracture mechanics principle and Castigliano's theorem. However, according to their computations, one crack disturbance function gets cancelled and disappears in the final vibration equation, while the other function seems to be constant along the beam; this function also tends to infinity along the neutral axis. Such crack disturbance functions could result in unrealistic displacements/stresses, which would not represent the displacements/stresses due to a crack. Later Chondros *et al.* [12] obtained the crack function for a simply supported beam (varying as a function of its distance from the crack), but the crack disturbance function is still infinite at the neutral axis, which would lead to infinite displacements/stresses.

This paper computes the change of strain energy due to the occurrence of a crack under dead-load (constant load) assumption, used in the energy balance approach to model crack growth. It considers the strain energy distribution along the cracked beam length by assuming an approximate function, which closely represents the high strain energy concentration around the crack tip. By modelling the strain energy variation along the beam length, the continuous equivalent bending stiffness and equivalent depth of the cracked beam are derived. Thereafter, the vibration for a beam with varying moment of inertia is obtained. The crack is assumed to be always open during vibrations. The natural frequencies are obtained using a four-term Galerkin's method. The frequency contours are plotted for crack detection.

2. ENERGY BALANCE IN A CRACKED BEAM UNDER DEAD-LOAD SITUATION

If the crack has propagated Δa, under a constant bending moment (due to dead-load loading assumption), the applied moment will perform some work W which will not only

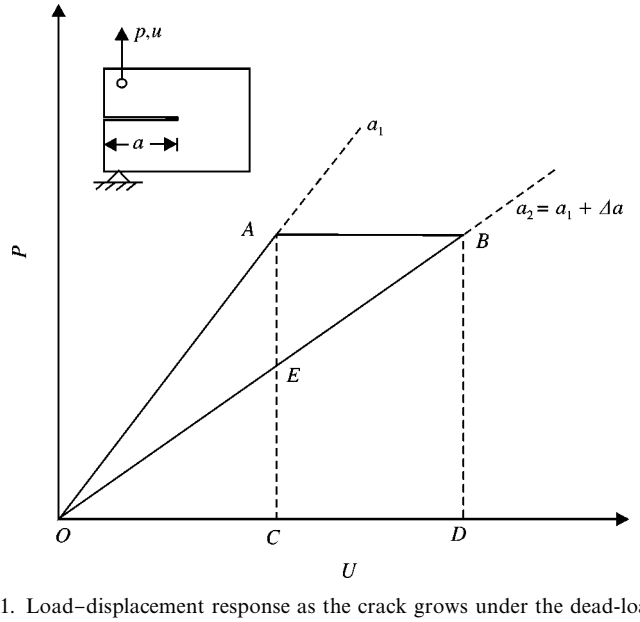

Figure 1. Load–displacement response as the crack grows under the dead-load loading.

assist the crack growth but also increase the structural strain energy [13]. Since the externally applied moment remains unaltered due to the crack growth Δa, using Clapeyron's theorem [13], the work W is twice the increase of elastic strain energy, and the final strain energy of the system is increased. Figure 1 shows the load–displacement response under dead-loading assumption for crack growth from a_1 and a_2. The energy before crack growth is represented by the area (OAC) and after the growth by the area (OBD). During crack growth (under the constant load P) the load P performs work given by the area $(ABCD)$. The increase of strain energy would by $(OBD) - (OAC) = (ABCD)/2$. Mathematical expressions are as follows:

$$W = E_c + \Delta U = 2\Delta U, \qquad E_c = \Delta U, \tag{1}$$

where E_c is energy for crack growth, and ΔU the increase of elastic strain energy in a cracked beam. The final strain energy of the cracked beam is

$$U_c = U + \Delta U = U + E_c, \tag{2}$$

where U is the strain energy of the beam prior to crack growth.

3. BENDING STIFFNESS OF THE BEAM WITH A CRACK

For the uncracked beam, subjected to a bending moment M, the strain energy in the beam is given by

$$U = \frac{1}{2}\int_0^1 \frac{M^2}{EI}\,\mathrm{d}x. \tag{3}$$

When a crack is formed on one side of the beam, and grows from zero to a under constant external bending moment, the energy consumed for crack growth, based on fracture mechanics, is

$$E_c = \int_0^a G\,\mathrm{d}A = \int_0^a Gb\,\mathrm{d}a, \tag{4}$$

where b is the width of the beam and G is the strain energy release rate. For the transverse vibration of the beam, the crack is mainly subjected to direct bending stresses and the shear stresses can be neglected; therefore, only the first mode crack exists. This gives the strain energy release rate as

$$G = \frac{K_I^2}{E}, \tag{5}$$

where K_I is the stress intensity factor for the first mode crack, and E is the Young's modulus. For a solid rectangular cross-section beam of depth h and width b, K_I is given as [13]

$$K_I = \frac{6M\sqrt{\pi a}}{bh^2}\,F(a), \tag{6}$$

where h is the depth of the beam; and for $a/h < 0{\cdot}6$,

$$F(a) = 1{\cdot}12 - 1{\cdot}4\left(\frac{a}{h}\right) + 7{\cdot}33\left(\frac{a}{h}\right)^2 - 13{\cdot}8\left(\frac{a}{h}\right)^3 + 14\left(\frac{a}{h}\right)^4. \tag{7}$$

Finally, using equation (4) the energy consumed in generating the crack becomes

$$E_c = D(a)M^2, \tag{8}$$

where

$$D(a) = \frac{18\pi[F(a)]^2 a^2}{Ebh^4}. \tag{9}$$

If EI_c is the bending stiffness of the cracked beam with the crack being always open, the final strain energy in the cracked beam could be alternatively expressed as

$$U_c = \frac{1}{2}\int_0^l \frac{M^2}{EI_c}\,\mathrm{d}x, \tag{10}$$

where I_c is the moment inertia of the cracked beam. It must be remembered that under the dead-load assumption, the external dynamic moment applied to the beam is constant over the length of the beam. For other cases, a suitable variation of bending moment along the length could be considered and the derivations modified.

From fracture mechanics considerations, the stresses/strains are highly concentrated around the crack tip, and reach the nominal stress at a location far away from the crack. So it can be assumed that the increase of strain energy due to crack growth, under constant applied moment, is concentrated mainly around the crack region. In order to represent mathematically the strain energy variation along the cracked beam length, the distribution of E_c (equal to the increase of strain energy) along the beam is postulated to be similar to

$$\frac{Q(a, c)}{1 + ((x - c)/k(a)a)^2}, \tag{11}$$

where $Q(a, c)$ and $k(a)$ are terms to be determined such that

$$E_c = \int_0^l \frac{Q(a, c)}{1 + ((x - c)/\{k(a)(a)\})^2}\,\mathrm{d}x \tag{12}$$

and c is the distance to the crack location from one end of the beam. Expression (11) has the maximum value at the crack location ($x = c$) and approaches zero far away from the crack. This makes the strain energy to be concentrated largely around the crack region. From equations (8) and (12), one obtains

$$Q(a, c) = \frac{D(a)M^2}{k(a)a[\arctan((l - c)/\{k(a)a\}) + \arctan(c/\{k(a)a\})]}. \tag{13}$$

Substitution of equations (3), (10) and (12) into equation (2) yields

$$\frac{1}{2}\int_0^l \frac{M^2}{EI_c}\,\mathrm{d}x = \frac{1}{2}\int_0^l \frac{M^2}{EI}\,\mathrm{d}x + \int_0^l \frac{Q(a, c)}{1 + ((x - c)/\{k(a)a\})^2}\,\mathrm{d}x. \tag{14}$$

From the above equation, the modified bending stiffness of the cracked beam is obtained as

$$EI_c = \frac{EI}{1 + EIR(a, c)/[1 + ((x - c)/\{k(a)a\})^2]}, \tag{15}$$

where

$$R(a, c) = \frac{2D(a)}{k(a)a[\arctan((1 - c)/\{k(a)a\}) + \arctan(c/\{k(a)a\})]}. \tag{16}$$

At the location of crack, i.e., at $x = c$, one has

$$h_c = h - a, \qquad \frac{EI}{EI_c} = \frac{bh^3/12}{bh_c^3/12} = \frac{bh^3/12}{b(h - a)^3/12}, \tag{17, 18}$$

where h_c is the equivalent height of the beam at the position of the crack. The EI_c given in equation (15) and the equivalent height (h_{eq}), computed thereby, will vary along the length of the beam. Using equations (15) and (18), one obtains

$$k(a) = \frac{3\pi[F(a)]^2(h - a)^3 a}{[h^3 - (h - a)^3]h}. \tag{19}$$

[The quantity $\{\arctan((1 - c)/\{k(a)a\}) + \arctan(c/\{k(a)a\})\}$ is approximately equal to π when the crack is not near the ends of the beam]. It can be seen that if no crack is present in the beam, i.e., $a = 0$, then the parameters $D(a) = 0$, $Q(a, c) = 0$, $R(a, c) = 0$ and $k(a) = 0$; from equation (15) the equivalent stiffness EI_c becomes the stiffness of the uncracked beam. The variations of normalized equivalent stiffness and normalized equivalent height of the cracked beam (along its length) are shown in Figure 2 [calculated from equation (15)].

To verify the reasonableness of energy distribution given in equations (2) and (11), the strain energy along the x-axis in a cracked plate (width of 40 units and unit thickness) under

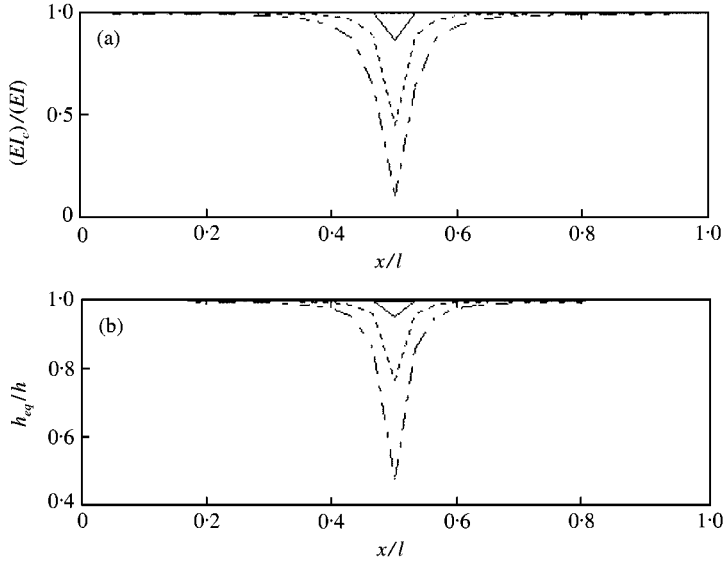

Figure 2. Variation of (a) normalized bending stiffness and (b) depth of a beam with a crack (crack location $c/l = 0{\cdot}5$): ——, $a/h = 0{\cdot}05$; - - - - -, $a/h = 0{\cdot}25$; – · – · –, $a/h = 0{\cdot}5$.

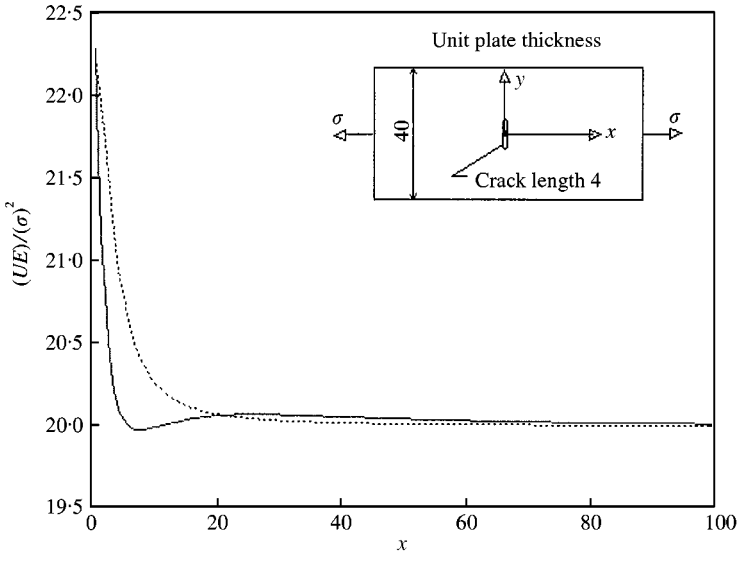

Figure 3. Energy distribution in x direction for a finite cracked plate (U—the strain energy over plate width, E—the elastic modulus): ——, elastic fracture mechanics theory; ------, theory developed in this paper.

uniform tension stress (plane stress) is calculated based on equations (2) and (11). At the same time, strain energy is computed numerically using Westergaard's method (complex functions) [14] in linear elastic fracture mechanics. The two curves of energy distribution are plotted in Figure 3, which are close to one another except near the crack zone. It can be seen from Figure 3 that, outside the crack influence zone, the energy distribution is nearly constant, and the increase of strain energy will be nearly zero (outside the crack influence zone), as is shown by both elastic fracture mechanics procedure and our procedure [assumption in equation (11)]. Thus, the increase of strain energy under dead-load is quite concentrated around the crack zone. Based on elastic fracture mechanics, the stresses near the crack tip tend to be very large or infinite, so does the strain energy. But, in reality, stresses and strain energy cannot approach infinity, and consequently plastic deformation occurs around the crack tip; therefore, the part of the increased strain energy under the dead-load is stored as plastic energy at the crack tip. This plastic strain energy is difficult to calculate. By using equations (11) and (12), the increase of strain energy is assumed to be concentrated around the crack tip, and the total energy increase is set to the correct value. The final strain energy distribution would then be a reasonable one. From Figure 3, the difference in energy between the exact solution and our approximate solution is marginal, and the energy concentration around the crack tip and the total increase of energy are also guaranteed by equations (11) and (12); therefore, the crack function represented by equation (11) is considered to be valid for the problem considered in this paper.

4. FORMULATIONS FOR A BEAM WITH TWO CRACKS

Under a constant external bending moment M, the energy supplied for two crack growths is

$$E_c = E_{c1} + E_{c2} = \int_0^{a_1} G_1 b \, \mathrm{d}a_1 + \int_0^{a_2} G_2 b \, \mathrm{d}a_2, \tag{20}$$

where a_1 and a_2 are the depths of two cracks, and G_1 and G_2 are the strain energy release rates for the two cracks. Similarly, for the transverse vibration of the beam, the first mode crack effect is dominant; and only the influence of the first mode crack is considered in this study,

$$G_1 = \frac{K_{I1}^2}{E}, \qquad G_2 = \frac{K_{I2}^2}{E}. \tag{21}$$

The two stress intensity factors are given as

$$K_{I1} = \frac{6M\sqrt{\pi a_1}}{bh^2} F_1(a_1), \qquad K_{I2} = \frac{6M\sqrt{\pi a_2}}{bh^2} F_2(a_2), \tag{22}$$

where for $a_1/h < 0{\cdot}6$ and $a_2/h < 0{\cdot}6$,

$$\begin{aligned} F_1(a_1) &= 1{\cdot}12 - 1{\cdot}4\left(\frac{a_1}{h}\right) + 7{\cdot}33\left(\frac{a_1}{h}\right)^2 - 13{\cdot}8\left(\frac{a_1}{h}\right)^3 + 14\left(\frac{a_1}{h}\right)^4, \\ F_2(a_2) &= 1{\cdot}12 - 1{\cdot}4\left(\frac{a_2}{h}\right) + 7{\cdot}33\left(\frac{a_2}{h}\right)^2 - 13{\cdot}8\left(\frac{a_2}{h}\right)^3 + 14\left(\frac{a_2}{h}\right)^4. \end{aligned} \tag{23}$$

Finally, equation (20) becomes

$$E_c = E_{c1} + E_{c2} = [D_1(a_1) + D_2(a_2)]M^2, \tag{24}$$

where

$$D_1(a_1) = \frac{18\pi[F_1(a_1)]^2 a_1^2}{Ebh^4}, \qquad D_2(a_2) = \frac{18\pi[F_2(a_2)]^2 a_2^2}{Ebh^4}. \tag{25}$$

Following the earlier derivations given in equation (8), for each crack growth, the energy consumed can be expressed by

$$E_{c1} = D_1(a_1)M^2, \qquad E_{c2} = D_2(a_2)M^2. \tag{26}$$

If the two cracks are not very close to each other so that the stress field for each crack could be treated separately using fracture mechanics theory, then the increase of strain energy due to crack growths under constant external bending moment could be assumed to be distributed in the beam according to the functions (similar to the case for one crack)

$$\frac{Q_1(a_1, c_1)}{1 + ((x - c_1)/\{k_1(a_1)a_1\})^2} \quad \text{and} \quad \frac{Q_2(a_2, c_2)}{1 + ((x - c_2)/\{k_2(a_2)a_2\})^2}, \tag{27}$$

where $Q_1(a_1, c_1)$, $Q_2(a_2, a_2)$ and $k_1(a_1)$, $k_2(a_2)$ are terms to be determined such that

$$E_{c1} = \int_0^l \frac{Q_1(a_1, c_1)}{1 + ((x - c_1)/\{k_1(a_1)a_1\})^2}\,\mathrm{d}x, \quad E_{c2} = \int_0^l \frac{Q_2(a_2, c_2)}{1 + ((x - c_2)/\{k_2(a_2)a_2\})^2}\,\mathrm{d}x \tag{28}$$

with c_1 and c_2 being distances to the crack locations from one end of the beam. Using equations (26) and (28), one obtains

$$Q_1(a_1, c_1) = \frac{D_1(a_1)M^2}{k_1(a_1)a_1[\arctan((l - c_1)/\{k_1(a_1)a_1\}) + \arctan(c_1/\{k_1(a_1)a_1\})]} \tag{29}$$

and

$$Q_2(a_2, c_2) = \frac{D_2(a_2)M^2}{k_2(a_2)a_2[\arctan((l - c_2)/\{k_2(a_2)a_2\}) + \arctan(c_2/\{k_2(a_2)a_2\})]}. \tag{30}$$

Substitution of equations (3), (10), (20), (24) and (28) into equation (2) yields

$$\frac{1}{2}\int_0^l \frac{M^2}{EI_c}\,\mathrm{d}x = \frac{1}{2}\int_0^l \frac{M^2}{EI}\,\mathrm{d}x + \int_0^l \frac{Q_1(a_1, c_1)}{1 + ((x - c_1)/\{k_1(a_1)a_1\})^2}\,\mathrm{d}x + \int_0^l \frac{Q_2(a_2, c_2)}{1 + ((x - c_2)/\{k_2(a_2)a_2\})^2}\,\mathrm{d}x. \tag{31}$$

From equation (31), the bending stiffness of the beam with two cracks is obtained as

$$EI_c = \frac{EI}{\dfrac{EIR_1(a_1, c_1)}{[1 + ((x - c_1)/\{k_1(a_1)a_1\})^2]} + \dfrac{EIR_2(a_2, c_2)}{[1 + ((x - c_2)/\{k_2(a_2)a_2\})^2]}}, \tag{32}$$

where

$$R_1(a_1, c_1) = \frac{2D_1(a_1)}{k_1(a_1)a_1[\arctan((1 - c_1)/\{k_1(a_1)a_1\}) + \arctan(c_1/\{k_1(a_1)a_1\})}, \tag{33}$$

$$R_2(a_2, c_2) = \frac{2D_2(a_2)}{k_2(a_2)a_2[\arctan((1 - c_2)/\{k_2(a_2)a_2\}) + \arctan(c_2/\{k_2(a_2)a_2\})}. \tag{34}$$

At the two crack locations, i.e., at $x = c_1$ and c_2 one has

$$\frac{EI}{EI_{c_1}} = \frac{bh^3/12}{b(h - a_1)^3/12}, \quad \frac{EI}{EI_{c_2}} = \frac{bh^3/12}{b(h - a_2)^3/12}, \tag{35}$$

where EI_{c_1} and EI_{c_2} are the equivalent bending stiffnesses at each of the crack positions respectively. Using equations (32) and (35), one obtains

$$k_1(a_1) = \frac{3\pi[F_1(a_1)]^2(h - a_1)^3 a_1}{[h^3 - (h - a_1)^3]h}, \quad k_2(a_2) = \frac{3\pi[F_2(a_2)]^2(h - a_2)^3 a_2}{[h^3 - (h - a_2)^3]h}. \tag{36}$$

[It is to be noted that $|c_1 - c_2| \gg a_1$ or a_2 when the two cracks are assumed to be not close together.]

The variations of normalized equivalent stiffness and depth (along the beam length) for two cracks are shown in Figure 4. It can be seen that the effect due to crack interaction is marginal unless the crack becomes large, viz., $a/h > 0{\cdot}5$. For more cracks on the beam, the same procedure could be utilized to compute the bending stiffness of the cracked beam, if the cracks do not interact considerably with one other.

5. TRANSVERSE VIBRATION EQUATIONS FOR CRACKED BEAMS

For an Euler beam, the vibration equation can be expressed using Newton's approach as

$$\frac{\mathrm{d}^2}{\mathrm{d}x^2}\left[EI_c\frac{\mathrm{d}^2 w}{\mathrm{d}x^2}\right] + m\frac{\partial^2 w}{\partial t^2} = 0, \tag{37}$$

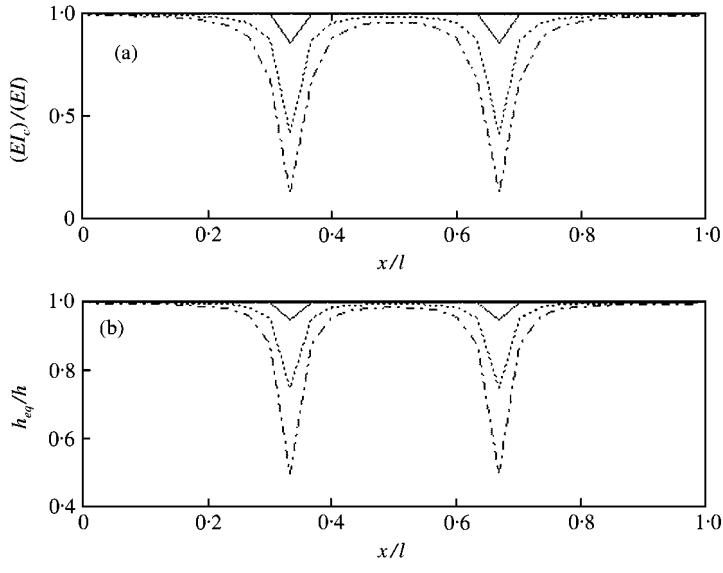

Figure 4. Variation of (a) normalized bending stiffness and (b) depth of a beam with two cracks (crack locations $c_1/l = 1/3$, $c_2/l = 2/3$): ——, $a/h = 0{\cdot}05$; - - - - -, $a/h = 0{\cdot}25$; – · – · –, $a/h = 0{\cdot}5$.

where m is the mass density along the beam length; in spite of the crack, the mass m per unit length will remain constant throughout the length of the beam.

Let $w = W(x)H(t)$, and substituting into the above equation (37), one obtains the characteristic equation as

$$\frac{\mathrm{d}^2}{\mathrm{d}x^2}\left[EI_c\frac{\mathrm{d}^2W}{\mathrm{d}x^2}\right] + m\omega_c^2 W = 0, \tag{38}$$

where ω_c is the natural frequency of the cracked beam.

To solve for natural frequencies and mode shapes, a four-term Galerkin's method is used. For a simply supported beam, the trial functions are selected as

$$W = C_1W_1 + C_2W_2 + C_3W_3 + C_4W_4, \tag{39}$$

where C_i are coefficients, and

$$W_1 = \sin(\pi x/l), \qquad W_2 = \sin(2\pi x/l), \qquad W_3 = \sin(3\pi x/l), \qquad W_4 = \sin(4\pi x/l). \tag{40}$$

The above four functions are the exact functions of the uncracked simply supported beam for the first four modes. For a fixed–fixed beam, the trial functions are selected [15], from the exact first four mode functions of the uncracked fixed beam, as

$$W = \sum_{i=1}^{4} C_iW_i, \tag{41}$$

where C_i are coefficients, and

$$W_i = \sin(p_ix/l) - \sinh(p_ix/l) + B_i[\cos(p_ix/l) + \cosh(p_ix/l)],$$

$$B_i = \frac{\cos(p_ix/l) - \cosh(p_ix/l)}{\sin(p_ix/l) + \sinh(p_ix/l)}, \tag{42}$$

$$p_1 = 4{\cdot}73, \quad p_2 = 7{\cdot}853, \quad p_3 = 10{\cdot}996, \quad p_4 = 14{\cdot}173. \tag{43}$$

TABLE 1

Frequency comparison for 4 *and* 8 *terms Galerkin's method* ($a/h = 0{\cdot}25$)

	Terms	First freq. ($*\sqrt{EI/\rho A}$)	Second freq. ($*\sqrt{EI/\rho A}$)	Third freq. ($*\sqrt{EI/\rho A}$)	Fourth freq. ($*\sqrt{EI/\rho A}$)
Simply supported beam	4	1·092224	4·337546	9·732307	17·368636
	8	1·092097	4·336085	9·728025	17·362530
	Relative diff. (%)	0·012	0·034	0·044	0·035
Fixed beam	4	2·483754	6·812762	13·281186	21·995036
	8	2·483727	6·811426	13·274610	21·985253
	Relative diff. (%)	0·0011	0·02	0·05	0·0445

TABLE 2

Frequency comparison for 4 *and* 8 *terms Galerkin's method* ($a/h = 0{\cdot}5$)

	Terms	First freq. ($*\sqrt{EI/\rho A}$)	Second freq. ($*\sqrt{EI/\rho A}$)	Third freq. ($*\sqrt{EI/\rho A}$)	Fourth freq. ($*\sqrt{EI/\rho A}$)
Simply supported beam	4	1·076682	4·188186	9·377521	16·952972
	8	1·074895	4·169363	9·332272	16·895126
	Relative diff. (%)	0·166	0·45	0·48	0·34
Fixed beam	4	2·471082	6·698606	12·891241	21·511597
	8	2·470662	6·681268	12·820941	21·421874
	Relative diff. (%)	0·017	0·26	0·55	0·42

To verify the convergence of Galerkin's method, more terms of trial functions are also used in the calculations. Tables 1 and 2 show the frequencies obtained by the four terms Galerkin's method and eight terms Galerkin's method for a cracked beam (one crack) with a crack depth ratio of $a/h = 0{\cdot}25$ and 0·5, respectively. The beam length is 3 m and the crack is located at $c/l = 0{\cdot}8$. The results indicate that the four terms Galerkin's method has given acceptable frequencies, with minimal errors.

6. EXPERIMENTS AND COMPARISON WITH THEORY

In order to verify the theory, vibration experiments for the cracked beam were carried out. The prismatic beam made of aluminum had a span length of 650 mm and a rectangular cross-section of $25{\cdot}4 \times 25{\cdot}4$ mm. Young's modulus of elasticity was $E = 62{\cdot}1$ GPa, and the material density was 2700 kg/m^3. The crack was introduced by making fine saw cuts at the middle of the beam and perpendicular to the longitudinal axis; this allowed the crack to remain open always. The beam was simply supported at two ends as shown in Figure 5. The excitation was carried out by an electrodynamic shaker at the center of the beam. Seven accelerometers were evenly placed on the beam. Dual Channel Signal Analyzer (type 2032) and the STAR analysis software [16] were used to extract the experimental results.

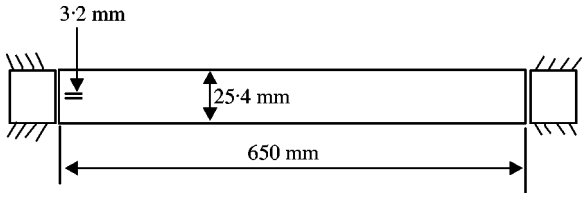

Figure 5. Simply supported experimental beam.

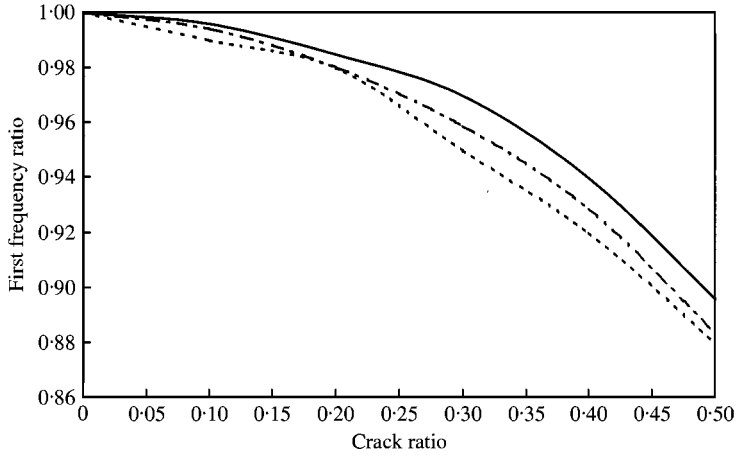

Figure 6. Comparison of experimental and theoretical values of frequency ratio: – – – –, reference [8]; ——, test; – · – · –, theoretical.

The beam without crack was first tested; then the crack was made in the beam from crack ratio $a/h = 0{\cdot}1$ to $0{\cdot}5$. For each crack ratio the beam was tested, and the frequency ratios, i.e., the ratio of the frequency of the cracked beam to that of the uncracked beam, were calculated. The frequency ratio against the crack ratio (first mode) is shown in Figure 6 and compared with our theoretical results and experimental data from Christides and Barr [8]. It can be seen that the theoretical and experimental results show a good agreement; the test results seem to be slightly lower than the theoretical values.

7. RESULTS AND DISCUSSIONS

The natural frequencies and mode shapes for transverse vibration of the cracked beams are calculated using the MATLAB program. The crack is assumed to be always open. All beams considered here are of a solid rectangular cross-section, with a depth of 0·2 m and a length of 3 m. For the simply supported beam with a crack, the first four frequencies are obtained for different crack depths and locations. When the crack is located at the midpoint of the beam, the normalized frequencies are shown for different crack depths in Figure 7. The frequencies decrease by about 11·6 and 8·2% for the first and third modes as the crack grows up to half the beam height. However, the frequencies change marginally for the second and fourth modes; this is due to the fact that the crack at the midpoint of the beam is located at the vibration nodes of the second and fourth modes. In reference [8], the fundamental frequency is shown to decrease by about 13%, theoretically, and 12%,

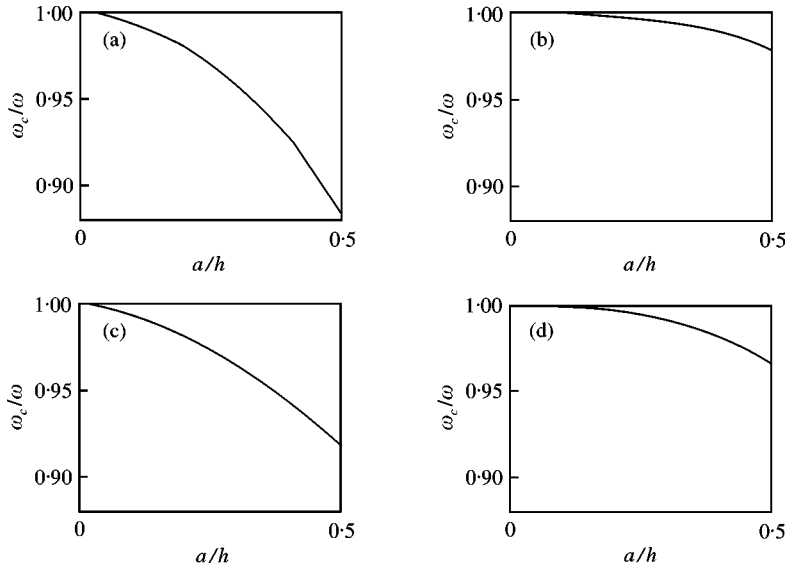

Figure 7. Variations of the first four frequencies as a function of crack depth for a simply supported beam (crack location $c/l = 0{\cdot}5$, ω_c/ω—frequency ratio): (a) mode one, (b) mode two, (c) mode three, (d) mode four.

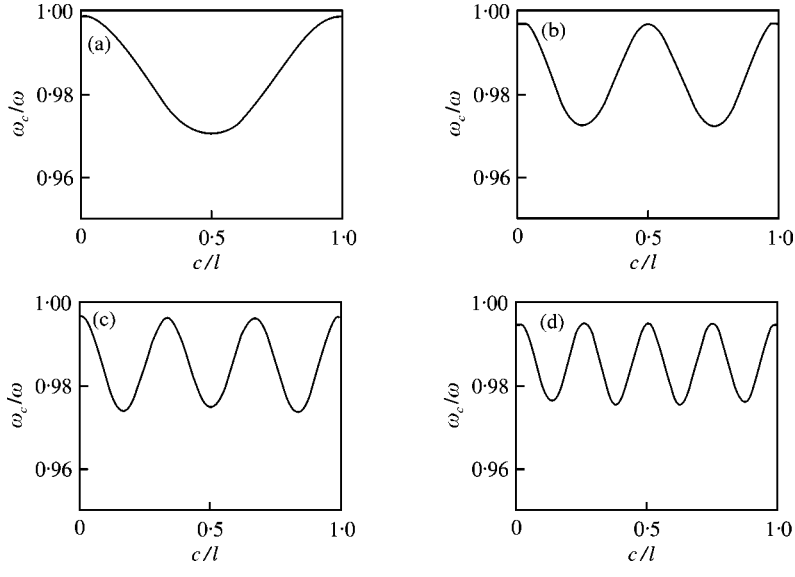

Figure 8. Variations of the first four frequencies as a function of crack location for a simply supported beam (crack depth ratio $a/h = 0{\cdot}25$): (a) mode one, (b) mode two, (c) mode three, (d) mode four.

experimentally, for a center-cracked simply supported beam with a crack depth of half the beam depth; these values are very close to the present results. Figure 8 shows the normalized frequencies for various crack locations when the crack depth is kept constant at $a/h = 0{\cdot}25$. As indicated in the figure, the crack occurring near the ends of the beam does not change the frequencies. For the first mode, the maximum change of frequency takes place as the crack occurs at the center. Generally, both the crack location and crack depth influence the natural frequencies of the cracked beam. The normalized frequencies versus crack

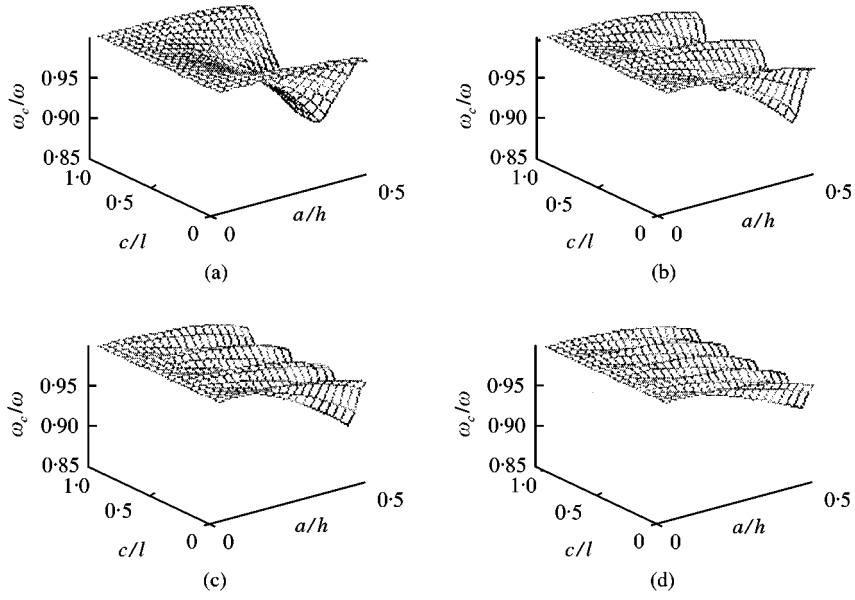

Figure 9. Frequencies versus crack locations and depths for a simply supported beam; (a) mode one, (b) mode two, (c) mode three, (d) mode four.

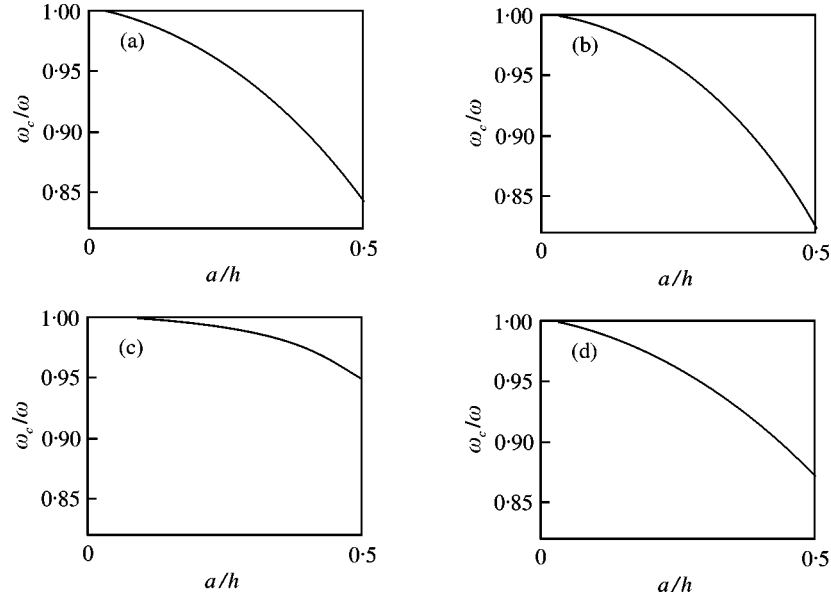

Figure 10. Variation of frequency as a function of crack depth for a simply supported beam with two cracks ($c_1/l = 1/3$, $c_2/l = 2/3$): (a) mode one, (b) mode two, (c) mode three, (d) mode four.

location and crack depth are shown in a three-dimensional plot in Figure 9. From these figures, it can be seen that the crack location and crack depth ratios are directly related to the frequency ratios. For a simply supported beam containing two cracks, which are located at $c_1/l = 1/3$ and $c_2/l = 2/3$ from the left end, the normalized frequencies are shown in Figure 10 as both cracks grow to a depth of $a/h = 0{\cdot}5$. The third mode has the smallest

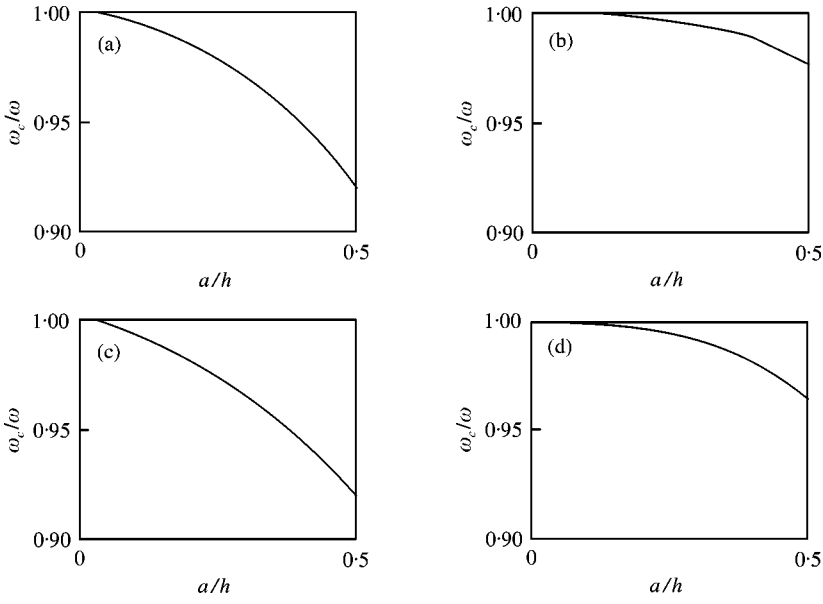

Figure 11. Variations of the first four frequencies as a function of crack depth for a fixed–fixed beam (crack location $c/l = 0{\cdot}5$): (a) mode one, (b) mode two, (c) mode three, (d) mode four.

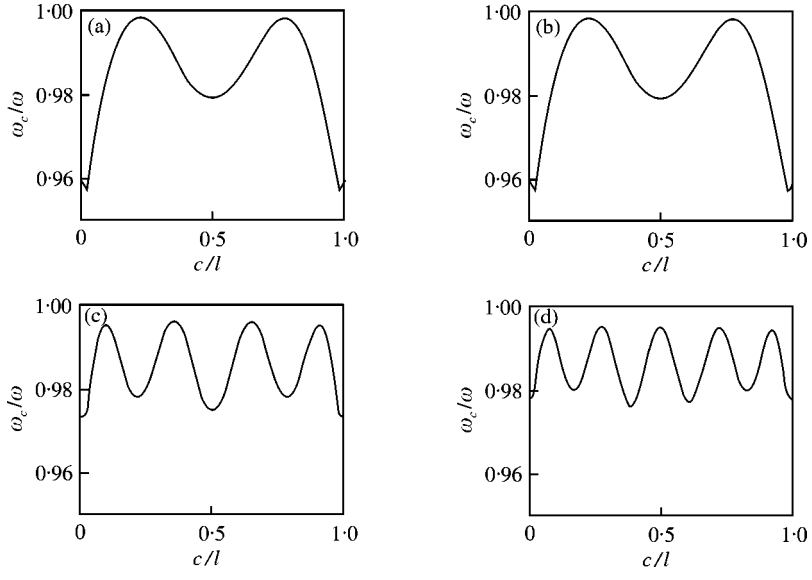

Figure 12. Variations of the first four frequencies as a function of crack location for a fixed–fixed cracked beam (crack depth ratio $a/h = 0{\cdot}25$): (a) mode one, (b) mode two, (c) mode three, (d) mode four.

change of frequencies (about 5%), while the other modes have much larger changes, which are 15·8, 17·5 and 13%, respectively; this is due to the fact that the nodes for the third mode are located near the crack location.

For a fixed–fixed beam containing a crack, Figure 11 shows the normalized frequencies for different crack depths when the crack is located at the midpoint of the beam. The changes of frequencies are similar to that for a simply supported beam. Figure 12 indicates

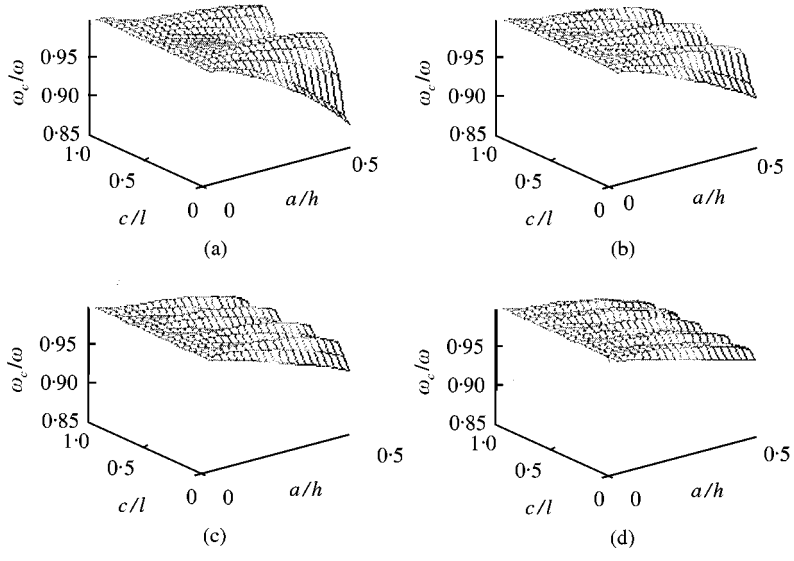

Figure 13. Frequencies versus crack depths and locations for a fixed–fixed beam: (a) mode one, (b) mode two, (c) mode three, (d) mode four.

the fluctuation of the normalized frequencies with crack depth $a/h = 0{\cdot}25$ as the crack location moves along the beam. Unlike the simply supported beam, the maximum changes of frequencies for the first and second modes occur near the ends of the beam. The reason is that the presence of a crack at these locations would reduce the stiffness near the supports (the boundary constraints). The three-dimensional plot of normalized frequency versus normalized crack location and depth are shown in Figure 13.

8. CRACK IDENTIFICATION PROCEDURE

As shown above, both crack location and depth have influences on the frequencies of the cracked beam. It turns out that one frequency could correspond to different crack depths and locations, as can be seen from Figures 9 and 13. Based on this, the contour line which has the same normalized frequency change (the same frequency change resulting from different combinations of crack depths and locations) can be plotted in a figure having the crack location and depth as its axes. Figure 14 shows contours for four modes of the simply supported beam with one crack, and Figure 15 shows contours for four modes of the fixed–fixed beam with one crack. To be clear and readable, the figures for each mode include only contours of two normalized frequency changes. The 0·98 contour means that the points on the curve have 2% decrease of frequency compared to the uncracked beam. The location and depth corresponding to any point on the curve would become the possible crack location and depth. A crack should and must belong to one contour line for each mode. The contour lines for different modes could be plotted together, and the intersection point(s) would indicate the crack location and crack depth. Since the frequencies could be measured accurately for low modes (for frequencies) and the contours for low modes tend to be simple, the contours for the first and second modes are plotted together to obtain the intersection point(s). If more than one intersection point is obtained, the contour for the third mode is also used to get the final point, which would indicate the crack location and

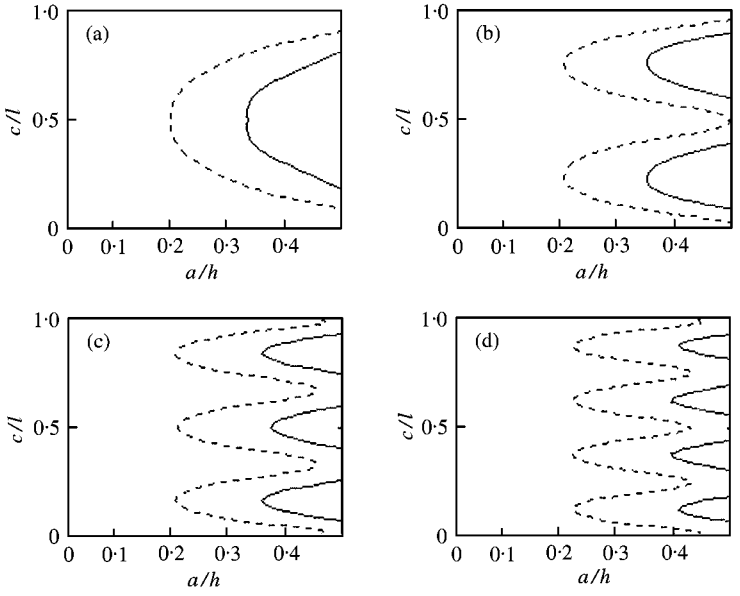

Figure 14. Frequency contours for a simply supported beam with a single crack: (a) mode one, (b) mode two, (c) mode three, (d) mode four: ——, $\omega_c/\omega = 0{\cdot}95$, - - - - -, $\omega_c/\omega = 0{\cdot}98$.

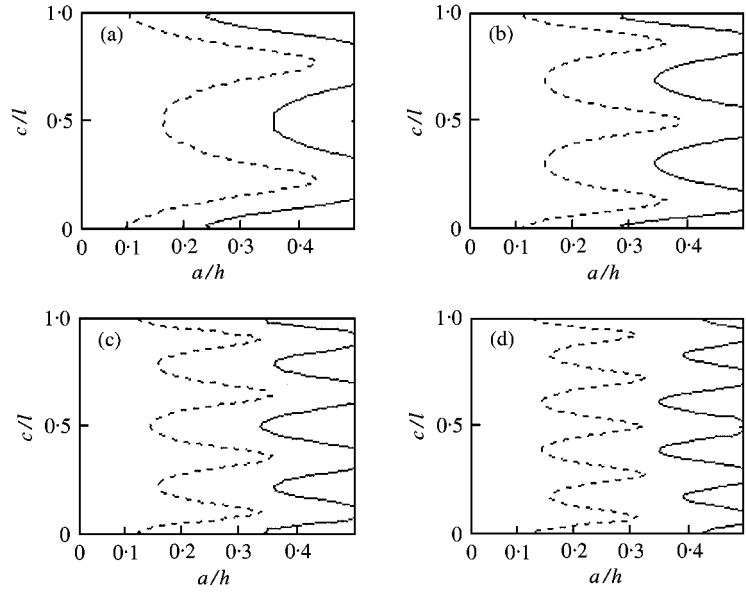

Figure 15. Frequency contours for a fixed–fixed beam with a single crack: (a) mode one, (b) mode two, (c) mode three, (d) mode four: ——, $\omega_c/\omega = 0{\cdot}96$, - - - - - -, $\omega_c/\omega = 0{\cdot}99$.

depth. If the crack location and vibration node coincide for a mode, the contour tends to disappear and no intersections are obtained; then the next mode is used. Basically, the first four frequencies are sufficient to identify the crack in the beam.

From the results in the above section a crack, with $a/h = 0{\cdot}25$, located at the middle of a simply supported beam, has the normalized frequencies of 0·9706 (i.e., a 2·94% decrease of

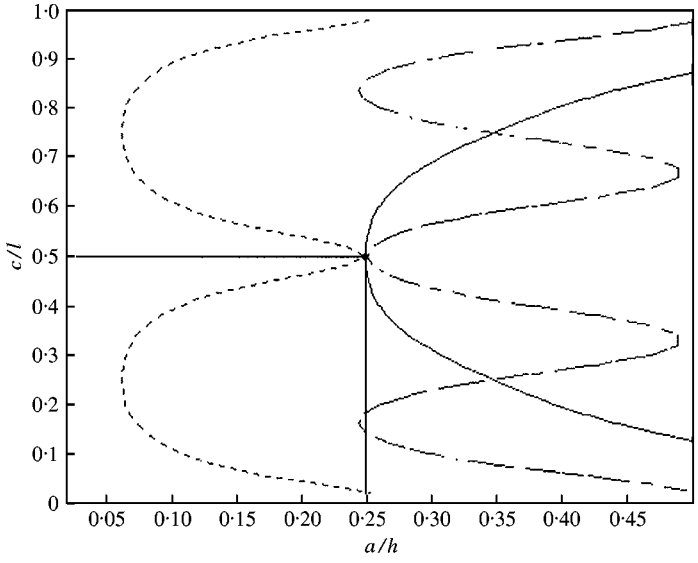

Figure 16. Crack identification by frequency contours from three different modes in a simply supported beam: ——, $\omega_c/\omega = 0{\cdot}9706$; - - - - -, $\omega_c/\omega = 0{\cdot}9972$; – · – · –, $\omega_c/\omega = 0{\cdot}9744$ (deduction: $a/h = 0{\cdot}25$, $c/l = 0{\cdot}5$).

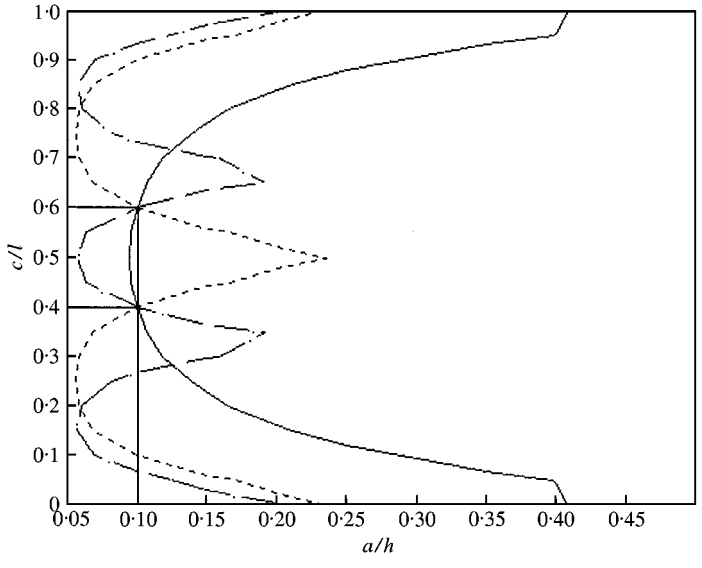

Figure 17. Crack identification by frequency contours from three different modes in a simply supported beam: ——, $\omega_c/\omega = 0{\cdot}9947$; - - - - -, $\omega_c/\omega = 0{\cdot}9979$; – · – · –, $\omega_c/\omega = 0{\cdot}9978$ (deduction: $a/h = 0{\cdot}1$, $c/l = 0{\cdot}4$ or $0{\cdot}6$).

frequency) for the first mode, 0·9744 for the third mode, and shows very small changes in frequencies for the other two modes (0·9972 and 0·994). The contour with the value of 0·9706 is retrieved from the first mode and is plotted in Figure 16 . The contour with the value of 0·9744 from the third mode is shown in the same figure. There are three intersection points for these two contours. Therefore, the contour from the second mode is also used to uniquely identify the crack location and depth. Three contours will give one intersection, which indicates the crack depth and location very well. To consider the situation of a non-central crack, the case of a simply supported beam with a crack depth $a/h = 0{\cdot}1$ and

located at $c/l = 0{\cdot}4$ is illustrated in Figure 17. The changes in the normalized frequencies for the above crack are, respectively, 0·9947, 0·9979 and 0·9978, for the first three frequencies. The 0·9947 contour for the first mode, 0·9979 contour for the second mode and 0·9978 contour for the third mode are shown in Figure 17. The intersection points indicate a crack depth $a/h = 0{\cdot}1$ and crack locations of $c/l = 0{\cdot}4$ or 0·6. Due to structural symmetry in the simply supported beam, the three contours would give two probable crack locations. The actual location can be identified by adding an off-center mass to the beam, which would make the vibration modes asymmetric.

9. CONCLUSIONS

The variation of the equivalent bending stiffness and depth (along the length) for a cracked beam are obtained using an energy-based model. Four modes are obtained for a simply supported beam and a fixed–fixed beam by selecting proper Galerkin's functions. Generally, the crack size will change the frequencies; however, the changes of frequencies are also dependent on the crack location. If the crack location coincides with the vibration node of one mode, the frequency for that mode remains almost unchanged. The crack near the ends would modify the boundary constraints, and thus decrease the frequencies significantly, as shown for the case of the fixed–fixed beam. The contour lines of frequency can be plotted for various modes for a beam containing the crack. The existing crack (in the beam) will belong to one particular contour in each mode. When these particular contours from different modes are plotted together, the intersection point(s) of the contours would provide the location and depth of the crack. Thus, the identification procedure developed in this study proves to be an elegant and simple one.

ACKNOWLEDGMENTS

The authors acknowledge the financial support from Research Grant awarded by Natural Science and Engineering Research Council, Canada. The help given by the Center for Computer Aided Engineering, Memorial University of Newfoundland is gratefully acknowledged.

REFERENCES

1. A. RYTTER 1993 *Ph.D. Thesis*, 46–50. *Department of Building Technology and Structural Engineering, University of Aalborg*. Vibration based inspection of civil engineering structures.
2. G. R. IRWIN 1960 *Structural Mechanics, Proceedings of First Symposium on Naval Structural Mechanics*. Oxford: Pergamon Press. Fracture mechanics.
3. H. OKAMURA, K. WATANABE and T. TAKAN 1972 *Progress in Flaw Growth and Fracture Toughness Testing, ASTM, STP* 536. Application of the compliance concept in fracture mechanics.
4. F. D. JU, M. AKGUN, E. T. WONG and T. L. LOPEZ 1982 *Productive Application of Mechanical Vibrations, American Society of Mechanical Engineers AMD* **52**, 113–126. Modal method in diagnosis of fracture damage in simple structures.
5. A. D. DIMAROGONAS and S. A. PAIPETIS 1983 *Analytical Methods in Rotor Dynamics*, 160–164. London: Elsevier Applied Science.
6. C. A. PAPADOPOULUS and A. D. DIMAROGONAS 1987 *Ingenieur-Archiv* **57**, 257–266. Coupling of bending and torsional vibration of a cracked Timoshenko shaft.
7. A. D. DIMAROGONAS 1996 *Engineering Fracture Mechanics* **55**, 831–857. Vibration of cracked structures: a state of the art review.

8. S. CHRISTIDES and A. D. S. BARR 1984 *International Journal Mechanics Science* **26**, 639–648. One-dimensional theory of cracked Bernoulli–Euller beams.
9. M.-H. H. SHEN and C. PIERRE 1994 *Journal of Sound and Vibration* **170**, 237–259. Free vibration of beams with a single-edge crack.
10. M.-H. H. SHEN and Y. C. CHU 1992 *Computers and Structures* **45**, 79–93. Vibrations of beams with a fatigue crack.
11. T. G. CHONDROS and A. D. DIMAROGONAS 1998 *Journal of Vibration and Acoustics* **120**, 742–746. Vibration of a cracked cantilever beam.
12. T. G. CHONDROS, A. D. DIMAROGONAS and J. YAO 1998 *Journal of Sound and Vibration* **215**, 17–34. A continuous cracked beam vibration theory.
13. E. E. GDOUTOS 1993 *Fracture Mechanics*, 79–91 and 53–56. Dordrecht: Kluwer Academic Publishers.
14. H. M. WESTERGAARD 1937 *Journal of Applied Mechanics* **6**, A.49–A.53. Bearing pressures and cracks.
15. D. J. GORMAN 1975 *Free Vibration Analysis of Beams and Shafts*, 1–14, New York: John Wiley and Sons, Inc.
16. STAR System Reference Manual 1994 Santa Clara, CA: GenRad, Inc.